PHYSICAL REVIEW B VOLUME 24, NUMBER 12 15 DECEMBER 1981

# Calculations of the electronic properties of hydrogenated silicon

D. A. Papaconstantopoulos
*Naval Research Laboratory, Washington, D. C. 20375*

E. N. Economou
*University of Crete, Crete, Greece*
(Received 16 July 1981)

We have used the coherent potential approximation to calculate the electronic densities of states for a model of hydrogenated amorphous silicon. The results demonstrate the restoration and widening of the band gap with increasing hydrogen content. In the valence band, excellent agreement with photoemission experiments is obtained. In the conduction band Si-H antibonding states are predicted that can be inferred from photoconductivity measurements.

## I. INTRODUCTION

### Basic experimental facts

The current intensive investigation of hydrogenated amorphous silicon originated in 1975 when Spear and LeComber[1] succeeded to substitutionally dope amorphous Si(*a*-Si), produced by decomposition of silane, through the incorporation of phosphorous and boron impurities. Soon after, it became apparent, as a result of work by Paul *et al.*[2] who also presented similar doping results in *a*-Si produced by sputtering in an Ar + H plasma, that the origin of the doping effects as well as other good electronic properties of this material[3,4] is the H passivation of dangling bonds. It has been shown recently,[5] for example, that the density of states in the middle of the gap can be reduced through hydrogenation to values as low as $5\times10^{14}$ $cm^{-3}eV^{-1}$. However, the amounts of hydrogen in these Si-H "alloys" were found to be as much as 100 times larger than the maximum number of dangling bonds. Therefore hydrogen, in addition to saturating the dangling bonds, introduces other changes in the electronic structure of *a*-Si.

Hydrogenation not only eliminates the dangling-bond states from the energy gap, but also widens the gap as demonstrated by Freeman and Paul,[6] by Cody *et al.*,[7] and by Goodman *et al.*[8] using different experimental techniques.

Away from the gap, photoemission measurements by von Roedern *et al.*[9] revealed hydrogen associated states well within the valence band. In the conduction band the photoconductivity data of Moustakas *et al.*[10] suggest the formation of Si-H antibonding states. The role of hydrogen in modifying the network is investigated through a variety of experimental techniques, such as infrared and Raman spectroscopy,[11,12] nuclear magnetic resonance,[13] small-angle x-ray scattering,[14] H implantation in *c*-Si,[15] and neutron scattering measurements.[16] For review of experimental work the reader is referred to the articles by Spear,[17] Moustakas,[3] and Fritzsche.[4]

### Present physical understanding

Unhydrogenated *a*-Si is thought of as a random network where the local tetrahedral arrangement, with bond lengths almost identical to those of the crystalline state, is retained to a high degree. An idealization of this concept is the so-called "ideal random network," where the tetrahedral coordination is satisfied throughout with very small fluctuations in the bond lengths and larger fluctuations in other longer range geometrical aspects such as ring sizes, dihedral angles, etc. This ideal random network defines the concept of topological disorder. In reality, there are important deviations from the ideal network, such as vacancies and other strong local distortions, which may even cluster together to form voids, internal surfaces, etc. Associated with this type of defect are dangling bonds (or, more generally, weakly bonded states). The number of these states is considerably smaller than

 

expected because the random lattice undergoes relaxation processes around a vacancy (or a cluster of vacancies) which result in a substantial bond reconstruction and, consequently, partial elimination of dangling-bond states. This "healing" process cannot be complete because of the high coordination[18,19] of Si which imposes severe geometrical restrictions on the reconstruction process.

Calculations for the ideal single-vacancy problem[20–22] show that dangling bonds are associated with local states whose eigenenergy lies in the gap (about 0.75 eV above the valence-band edge). Allowing the atoms around the ideal vacancy to relax pushes these states toward the valence and the conduction band. On the basis of these calculations, one can conclude that the dangling bonds, which have survived reconstruction, create states in the gap. These states are of the order of $10^{19}-10^{20}$ $cm^{-3}eV^{-1}$ as electron-spin-resonance experiments show.[11,12] It is generally believed that hydrogen passivates the dangling-bond states by forming Si—H bonds which are associated with states lying well within the valence band. Furthermore, if the material is grown in the presence of hydrogen, much of the reconstruction is prevented as a result of Si—H bond formation.[3] This explains why the highest amount of hydrogen in $a$-$SiH_x$ is so much larger than the number of dangling bonds (which survived reconstruction) in the unhydrogenated specimens. One may view the abundant presence of hydrogen during the growth process as effectively reducing the coordination of the resulting structure and thus allowing the growth of an unstrained, chemically stable substance. The widening[6–8] of the gap upon hydrogenation has been attributed to the stronger Si—H bond as compared with the Si—Si bond. Here, as well as in a preliminary report[23,24] of this work, we argue that an equally important contribution comes from the effective reduction of the $pp\pi$ interaction upon hydrogenation.

## Theoretical models

From the above discussion it follows that a complete theory of hydrogenated $a$-Si has to deal with the following aspects of the problem.

(*a*) *Topological disorder.* Models incorporating topological disorder (TD) using a continuous random network, have been used[25,26] in conjunction with the orthogonalized-linear-combination-of-atomic-orbitals method to perform calculations of the electronic structure of $a$-Si:H. These calculations are consistent with photoemission experiments,[9] but they do not seem capable of obtaining detailed information for the densities of states (DOS) in the gap region and in the conduction band. Recently, Cohen *et al.*[27] argued that TD widens the gap and creates a tail in the DOS which enters the gap. Using small Si-H molecules terminated by Si Bethe lattices, Allan and Joannopoulos[28] have examined the question of ring statistics and its influence on certain regions of the spectrum. We feel that increasing hydrogenation may reduce the importance of ring statistics. Finally, TD, introduced by allowing variation in the dihedral angle, seems to effectively reduce the size of the $pp\pi$ interaction[23] and thus contributes further to the widening of the gap.

(*b*) *Reconstruction.* Reconstruction is probably the most important aspect of unhydrogenated $a$-Si. A qualitative lattice distortion model has been proposed by Watkins.[29] This model has been used as the basis to address the problem of the single reconstructed vacancy in Si using elaborate Green's-function techniques.[30,31] Also, White and Ngai[32] have discussed reconstructing states at the Si-$SiO_2$ interface. However, it seems that the amount of reconstruction, and therefore its importance, is reduced when hydrogen is present during the growth process.[3] Thus, depending on the abundance of hydrogen, the method of preparation, and other details of the growth process, the importance of reconstruction may vary from a dominant role to an insignificant detail.

(*c*) *Chemical nature and statistics of the hydrogen incorporation.* By chemical nature we mean whether the hydrogen is always bonded to one of the four $sp^3$ hybrids of Si, or may participate in other bonding configurations. Even if hydrogen is only bonded to Si one still has to know statistical information such as the percentage of monohydrides versus polyhydrides, whether or not there are some hydrogen clustering tendencies, etc. Obviously, these questions affect the electronic structure of the material.

With the exception of the continuous-random-network work,[25,26] most attempts in the literature to study the above three aspects are based on considering small Si-H molecules. These Si-H clusters are either isolated or terminated by hydrogen[33] or by Si Bethe lattice[28] to avoid unphysical boundary effects. These approaches are very useful in revealing certain qualitative and even semiquantitative aspects of the subject; they are also necessary in some cases (e.g., other hydrogen bonding config-

urations) given the difficulty of the problem. However, these approaches cannot be considered as a substitute for calculations dealing with macroscopic size systems. We should not lose sight of the fact that these calculations more properly apply to the study of Si-H molecules than to the Si-H solid. In addition, the Bethe-lattice calculations are based on a first-nearest-neighbor interaction Hamiltonian which, as has been shown,[22,34] is inadequate to reproduce the correct gap or a reasonable conduction band.

The work we report here is one of the first attempts to deal with the problem at the actual macroscopic scale which involves many particular local configurations. We found it necessary to omit aspects related to topological disorder and reconstruction, and concentrate our efforts on the third aspect which is the role of hydrogen in the electronic structure of $a$-$SiH_x$. We think that for fully hydrogenated samples with high hydrogen content, hydrogenation is the most important aspect and that TD and reconstruction will change our results only quantitatively. To treat the role of hydrogen, we have used a particular model of hydrogen incorporation which assumes that all hydrogens are bonded to Si. Although our model may not be quite realistic, we think that it incorporates the important features (which are independent of particular models) such as bonding and antibonding states made out of Si $sp^3$ and hydrogen orbitals, a stronger Si—H bond (as compared with Si—Si bond) which affects the states at the bottom of the conduction band, and an effective reduction, with hydrogenation, of the $pp\pi$ interaction which is very important for the states at the top of the valence band.

Thus we believe that the main conclusions of our work have a much wider validity than the particular model from which they were derived. Recently, a calculation complementary to ours was reported by Pickett.[35] Pickett has employed the self-consistent pseudopotential method with a supercell configuration to study the electronic states of the hydrogen-saturated vacancy in Si. His approach differs from ours in that he is using a periodic array of atoms, while we are using a random array. The results of the two calculations, however, have the same qualitative features. In the Appendix we utilize his conclusion of a strong Si—H bond and his charge-density contours to estimate certain H-Si matrix elements of our tight-binding Hamiltonian. Finally, we refer to a calculation along similar lines to ours reported by Divincenzo *et al.*[36] This calculation deals with a model defect which is an isolated monovacancy in an otherwise perfect crystal.

The rest of the paper is organized as follows. Section II describes our model configuration of hydrogenated $a$-Si; Sec. III gives the theory of the coherent-potential approximation as applied in the present work; Sec. IV discusses the results and compares with experiment, and the Appendix deals with the estimation of the H-H and H-Si matrix elements.

## II. THE PRESENT MODEL

Our model describes hydrogenated Si by constructing an effective lattice whose sites may have probability $c$ of being vacant and probability 1-$c$ of having a Si atom. In addition, we have assumed that hydrogen atoms may be located along the lines connecting a vacant site with its nearest neighbors, as shown in Fig. 1(b). Thus we have included in our model, at random, Si sites, vacancy sites, and sites that have one, two, three, or four hydrogen atoms. Using this model of disorder, we have used a tight-binding form of the coherent-potential approximation[37,38] (CPA) to perform detailed calculations of the electronic DOS.

The starting point of the present calculations is a Slater-Koster (SK) Hamiltonian $H$; the bases are four Si orbitals (one $|s\rangle$ and three $|p\rangle$) which have been taken as orthonormal. The matrix elements in this basis have been chosen in such a way as to reproduce the band structure of crystalline Si (both valence and conduction band) rather accurately.[22] Such an accuracy is necessary in order to study dangling-bond states. As we have discussed in the Introduction, we have neglected the TD except for the following point: Because the dihedral angle (i.e., the angle which determines the orientation of the three bonds which are attached to one end of a given bond with respect to the other three bonds which are attached to the other end of this given bond) varies in a disordered structure in a range which starts from the eclipsed configuration all the way to the staggered configuration, the $pp\pi$ interaction fluctuates. As we have mentioned before, the $pp\pi$ interaction is very important because it controls the position of the top of the valence band. In the periodic case, the $pp\pi$ interaction is equal to the difference $\Delta = E_{x,y}(\frac{1}{2}\frac{1}{2}\frac{1}{2}) - E_{x,x}(\frac{1}{2}\frac{1}{2}\frac{1}{2}) = \gamma_6 - \gamma_5$, where $\gamma_6 = \langle 6|H|2\rangle$ and $\gamma_5 = \langle 6|H|3\rangle = \langle 6|H|4\rangle$ and $|2\rangle$, $|3\rangle$,

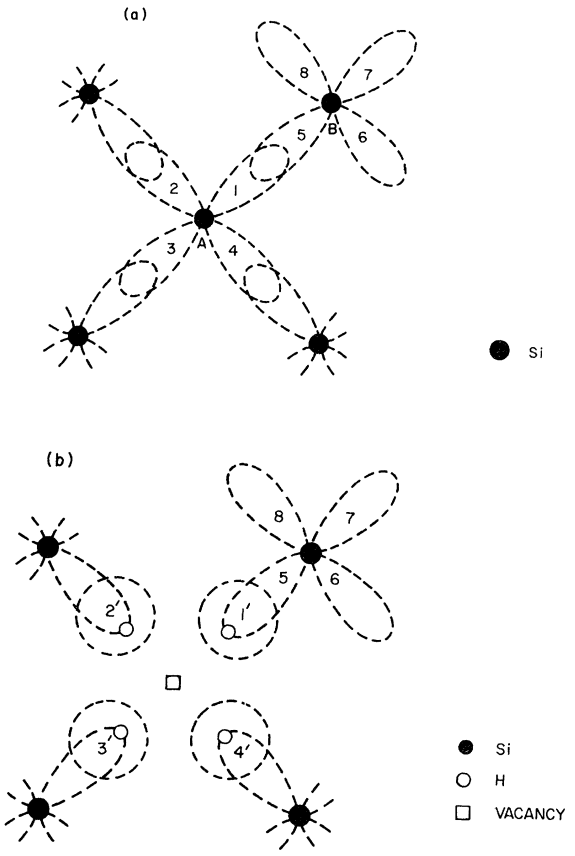


FIG. 1. (a) Two-dimensional view of the atom configuration for Si showing the $sp^3$ orbitals. (b) Two-dimensional view of the atom configuration for Si-H showing the replacement of one Si atom by four H atoms.

$|4\rangle$, and $|6\rangle$ are the $sp^3$ hybrids shown in Fig. 1(a). In the random structure $\langle 6|H|3\rangle \neq \langle 6|H|4\rangle$ so that, in general, there are three different matrix elements $\langle 6|H|2\rangle$, $\langle 6|H|3\rangle$, and $\langle 6|H|4\rangle$. We have found how these matrix elements vary with the dihedral angle and we have taken, as a measure of the $pp\pi$ interaction, the average of the maximum of the three differences of one of them from the mean value of the other two. To perform the average, we have assumed that the dihedral angle has a uniform (constant) probability distribution. The effect of this is to change the matrix elements $E_{x,y}(\frac{1}{2}\frac{1}{2}\frac{1}{2})$ and $E_{x,x}(\frac{1}{2}\frac{1}{2}\frac{1}{2})$ from their crystalline values[22] 1.407 and 0.276 eV, respectively, to the values 1.39 and 0.31 eV. This reduces the $pp\pi$ interaction $\Delta$ from the value 1.131 eV to the value 1.08 eV. This leads to a recession of the top of the valence band and, hence, a widening of the gap from $E_g = 1.0$ eV in the crystalline case to 1.05 in the "amorphous" state. We believe that if TD were taken into account in a more rigorous way, it would lead to a more substantial widening of the gap and to a tailing of the states into the gap.

Our model also omits reconstruction; this is a very serious omission in the cases where the dangling bonds have not been passivated by hydrogen. For those cases, our results should not be taken seriously except to say that if all these dangling bonds were present there would be substantial DOS in the gap. On the other hand, in the fully hydrogenated cases we expect that reconstruction is minimal and thus its omission in our model is not a serious shortcoming.

The way hydrogen is incorporated in our model is shown in Fig. 1(b), where an ideal vacancy has been created, resulting in four $sp^3$ Si dangling bonds. Such vacancies can accommodate up to four hydrogen atoms as shown in Fig. 1(b). The result of replacing a Si by four hydrogens as shown in Fig. 1(b) is to replace the Si-Si matrix elements [given in Table I of Ref. 22 with $E_{x,y}(\frac{1}{2}\frac{1}{2}\frac{1}{2})$ and $E_{x,x}(\frac{1}{2}\frac{1}{2}\frac{1}{2})$ changed as discussed above] by H-H or H-Si matrix elements. In the Appendix we explicitly estimate the effective matrix elements associated with the configuration of Fig. 1(b). They are the following:

$$E'_{s,s}(000) = -8.72 \text{ eV}, \quad E'_{x,x}(000) = -1.6 \text{ eV},$$

$$E'_{s,s}(\tfrac{1}{2}\tfrac{1}{2}\tfrac{1}{2}) = -3.05 \text{ eV}.$$

$$E'_{s,x}(\tfrac{1}{2}\tfrac{1}{2}\tfrac{1}{2}) = 1.96 \text{ eV}, \quad E'_{x,x}(\tfrac{1}{2}\tfrac{1}{2}\tfrac{1}{2}) = 0.64 \text{ eV},$$

$$E'_{x,y}(\tfrac{1}{2}\tfrac{1}{2}\tfrac{1}{2}) = 0.98 \text{ eV}.$$

Actually, the second- and third-nearest-neighbor matrix elements will be affected by the replacement of a Si by four hydrogens. We assumed that this additional modification is much less significant than the diagonal and first-nearest-neighbor changes and thus we have omitted it. It must be pointed out that the $E'(000)$'s given above are matrix elements between fictitious $s$ and $p$ orbitals associated with the four hydrogens shown in Fig. 1(b) (they are the same linear combinations of the hydrogen orbitals $|1'\rangle$, $|2'\rangle$, $|3'\rangle$, and $|4'\rangle$ as the actual Si, $s$, and $p$ are of the corresponding four $sp^3$ hybrids; see Appendix) and the $E'(\frac{1}{2}\frac{1}{2}\frac{1}{2})$'s are matrix elements between the fictitious four hydrogen $s$ and $p$'s and the $s$ and $p$'s of the nearest Si's.

## III. COHERENT-POTENTIAL APPROXIMATION

As we have mentioned in the previous section, we have used the tight-binding (TB) CPA (Refs. 37 and 38) to obtain the DOS. Since, in addition to the configuration shown in Fig. 1(b), we have also considered cases where one or more of the hydrogens shown are missing, we had to generalize the TB-CPA to handle these additional configurations. The CPA condition of zero scattering on the average leads, in our case to the following equation:

$$(1-c)\tilde{U}_{\mathrm{Si}}(1-\tilde{G}_e\tilde{U}_{\mathrm{Si}})^{-1}+x_v\tilde{U}_v(1-\tilde{G}_e\tilde{U}_v)^{-1}+\frac{x_1}{4}\sum_{i=1}^{4}\tilde{U}_{1i}(1-\tilde{G}_e\tilde{U}_{1i})^{-1}+\frac{x_2}{6}\sum_{i=1}^{6}\tilde{U}_{2i}(1-\tilde{G}_e\tilde{U}_{2i})^{-1}$$
$$+\frac{x_3}{4}\sum_{i=1}^{4}\tilde{U}_{3i}(1-\tilde{G}_e\tilde{U}_{3i})^{-1}+x_4\tilde{U}_4(1-\tilde{G}_e\tilde{U}_4)^{-1}=0\ , \tag{1}$$

where $\tilde{G}_e$ is an effective Green's function obtained from the corresponding crystalline Si Green's function $\tilde{G}$ by replacing $\epsilon_s$ and $\epsilon_p$ with the CPA self-energies $\Sigma_s$ and $\Sigma_p$, respectively. From Ref. 22 we have that $\epsilon_s \equiv E_{s,s}(000) = -3.953$ eV and $\epsilon_p \equiv E_{x,x}(000) = 1.512$ eV. $\tilde{G}(E)$ is a $4\times4$ diagonal matrix with matrix elements $G_{11}, G_{22}, G_{22}, G_{22}$, and where $G_{11} = \langle 0s \,|\, (E-H)^{-1} \,|\, 0s \rangle$ and $G_{22} = \langle 0x \,|\, (E-H)^{-1} \,|\, 0x \rangle$, where $|\,0s\,\rangle$ and $|\,0x\,\rangle$ are the $s$ and $p_x$ Si orbitals at the site 0, and where $\tilde{U}_{\mathrm{Si}}$, the Si scattering matrix, is

$$\tilde{U}_{\mathrm{Si}} = \begin{bmatrix} \epsilon_s-\Sigma_s & 0 & 0 & 0 \\ 0 & \epsilon_p-\Sigma_p & 0 & 0 \\ 0 & 0 & \epsilon_p-\Sigma_p & 0 \\ 0 & 0 & 0 & \epsilon_p-\Sigma_p \end{bmatrix} . \tag{2}$$

$\tilde{U}_v$, the vacancy scattering matrix is

$$\tilde{U}_v = \begin{bmatrix} \infty & 0 & 0 & 0 \\ 0 & \infty & 0 & 0 \\ 0 & 0 & \infty & 0 \\ 0 & 0 & 0 & \infty \end{bmatrix} . \tag{3}$$

$\tilde{U}_{1i}$ is a matrix corresponding to the four equivalent configurations where only one hydrogen atom is present with probability of occurrence $x_1/4$,

$$\tilde{U}_{11} = \tilde{S}\begin{bmatrix} \gamma_1' & 0 & 0 & 0 \\ 0 & \infty & 0 & 0 \\ 0 & 0 & \infty & 0 \\ 0 & 0 & 0 & \infty \end{bmatrix}\tilde{S}-\tilde{\Sigma}\ , \tag{4}$$

and, similarly, for $\tilde{U}_{12}$, $\tilde{U}_{13}$, and $\tilde{U}_{14}$. $\tilde{S}$ is the matrix which accomplished the orbital transformation (Appendix). The hydrogen matrix element $\gamma_1'$ is taken equal to $-3.38$ eV which is its value for silane (Appendix). The matrix $-\tilde{\Sigma}$ is a diagonal matrix like (2) but without the $\epsilon_s$ and $\epsilon_p$. $\tilde{U}_{2i}$ is a matrix corresponding to the six equivalent configurations where two hydrogen atoms are present with probability $x_2/6$,

$$\tilde{U}_{21} = \tilde{S}\begin{bmatrix} \gamma_1' & \gamma_2' & 0 & 0 \\ \gamma_2' & \gamma_1' & 0 & 0 \\ 0 & 0 & \infty & 0 \\ 0 & 0 & 0 & \infty \end{bmatrix}\tilde{S}-\tilde{\Sigma}\ , \tag{5}$$

and similarly for $\tilde{U}_{22}$, $\tilde{U}_{23}$, $\tilde{U}_{24}$, $\tilde{U}_{25}$, and $\tilde{U}_{26}$. The matrix element $\gamma_2' = -1.78$ eV is estimated in the Appendix. $\tilde{U}_{3i}$ is a matrix corresponding to the four equivalent configurations where three hydrogen atoms are present with probability $x_3/4$,

$$\tilde{U}_{31} = \tilde{S}\begin{bmatrix} \gamma_1' & \gamma_2' & \gamma_2' & 0 \\ \gamma_2' & \gamma_1' & \gamma_2' & 0 \\ \gamma_2' & \gamma_2' & \gamma_1' & 0 \\ 0 & 0 & 0 & \infty \end{bmatrix}\tilde{S}-\tilde{\Sigma}\ , \tag{6}$$

and similarly for $\tilde{U}_{32}$, $\tilde{U}_{33}$, and $\tilde{U}_{34}$. $\tilde{U}_4$ is a matrix corresponding to the case of four hydrogen atoms present with probability $x_4$:

$$\tilde{U}_4 = \tilde{S}\begin{bmatrix} \gamma_1' & \gamma_2' & \gamma_2' & \gamma_2' \\ \gamma_2' & \gamma_1' & \gamma_2' & \gamma_2' \\ \gamma_2' & \gamma_2' & \gamma_1' & \gamma_2' \\ \gamma_2' & \gamma_2' & \gamma_2' & \gamma_1' \end{bmatrix}\tilde{S}-\tilde{\Sigma}\ . \tag{7}$$

The probability of occurrence of the configuration shown in Fig. 1(a) is denoted by $1-c$; the probability of the configuration of Fig. 1(b) is denoted by $x_4$. Obviously,

$$c = x_0+x_1+x_2+x_3+x_4\ . \tag{8}$$

In the case where there is no statistical correlation among hydrogens the probabilities $x_i$ $(i=0,\ldots,4)$ can be expressed in terms of the quantity $x$, which is the ratio of the total number of hydrogens over the total number of lattice sites, and the quantity $c$:

$$x_l = c\frac{4!}{(4-l)!l!}\frac{x^l(4c-x)^{4-l}}{(4c)^4}, \quad l=0,\ldots,4 . \tag{9}$$

The case $x=4c$ represents the fully hydrogenated case where $x_4=c$ and $x_l=0$, $l=0,\ldots,3$; this is the case where the reconstruction effects are expected to be minimal and, consequently, our model to be more realistic.

Since the Green's function $\tilde{G}_e$ is a function of the self-energy $\tilde{\Sigma}$, the CPA condition [Eq. (1)] is very complicated to solve, even numerically. For this reason we have solved Eq. (1) for the limiting cases $x=0$ (no hydrogen) and $x=4c$ (all vacancies saturated by hydrogen). For $x=0$, Eq. (1) combined with Eq. (3) reduces to

$$(1-c)\tilde{U}_{\mathrm{Si}}(1-\tilde{G}_e\tilde{U}_{\mathrm{Si}})^{-1}-c\tilde{G}_e^{-1}=0 . \tag{10}$$

Utilizing symmetry Eq. (10) results in the following two scalar equations:

$$\Sigma_s=\epsilon_s-c/G_{11}(E,\Sigma_s,\Sigma_p) ,$$
$$\Sigma_p=\epsilon_p-c/G_{22}(E,\Sigma_s,\Sigma_p) . \tag{11}$$

Equations (11) are solved simultaneously for $\Sigma_s$ and $\Sigma_p$ using a Newton-Raphson iterative procedure. The Brillouin-zone summation necessary in evaluating $G_{11},G_{22}$ was done for 240 $k$ points in the irreducible zone.

For $x=4c$, Eq. (1) reduces to the following expressions:

$$G_{11}\Sigma_s^2+(1-\epsilon_sG_{11}-\epsilon_s'G_{11})\Sigma_s-c(\epsilon_s'-\epsilon_s)-\epsilon_s+\epsilon_s\epsilon_s'G_{11}=0 , \tag{12}$$
$$G_{22}\Sigma_p^2+(1-\epsilon_pG_{22}-\epsilon_p'G_{22})\Sigma_p-c(\epsilon_p'-\epsilon_p)-\epsilon_p+\epsilon_p\epsilon_p'G_{22}=0 ,$$

where $\epsilon_s'=E_{s,s}'(000)=-8.72$ eV and $\epsilon_p'=E_{x,x}'(000)=-1.6$ eV are the effective H-H matrix elements (Appendix). Equations (12) are also solved for $\Sigma_s$ and $\Sigma_p$ by iteration. Since both sets of Eqs. (11) and (12) are complex, we found it computationally efficient to separate them into their real and imaginary parts and do the computer code in real arithmetic.

For the intermediate values of $x$, we have employed an average $t$-matrix approximation (ATA) instead of the CPA. We have done this to simplify the computational effort since the additional errors are small, and because the cases with $x<4c$ are not very realistic due to the reconstruction that takes place. The ATA-like approximation used for $0<x<4c$ is the following. We define $\Sigma_i(E;x)$ $i=s,p$ by the relation

$$\Sigma_i(E;x)=\left[1-\frac{x}{4c}\right]\Sigma_i(E;0)+\frac{x}{4c}\Sigma_i(E;4c) , \tag{13}$$

where $\Sigma_i(E;0)$ and $\Sigma_i(E;4c)$ have been obtained from the CPA described above.

Having determined $\Sigma_s$ and $\Sigma_p$ [using the CPA condition (1) for the cases $x=0,4c$ and Eq. (13) for $x\neq 0,4c$] we can obtian $\tilde{G}_e(E)$; then in all cases the DOS is given from the following expressions:

$$N_{\mathrm{Si}}=\frac{(1-c)}{\pi}\{-\mathrm{Im\,Tr}[(1-\tilde{G}_e\tilde{U}_{\mathrm{Si}})^{-1}\tilde{G}_e]\} ,$$
$$N_{\mathrm{H}}=\frac{x_1}{4\pi}\sum_{i=1}^{4}\{-\mathrm{Im\,Tr}[(1-\tilde{G}_e\tilde{U}_{1i})^{-1}\tilde{G}_e]\}+\frac{x_2}{6\pi}\sum_{i=1}^{6}\{-\mathrm{Im\,Tr}[(1-\tilde{G}_e\tilde{U}_{2i})^{-1}\tilde{G}_e]\}$$
$$+\frac{x_3}{4\pi}\sum_{i=1}^{4}\{-\mathrm{Im\,Tr}[(1-\tilde{G}_e\tilde{U}_{3i})^{-1}\tilde{G}_e]\}+\frac{x_4}{\pi}\{-\mathrm{Im\,Tr}[(1-\tilde{G}_e\tilde{U}_4)^{-1}\tilde{G}_e]\} , \tag{14}$$

where the notation is the same as that of Eq. (1).

In the special case of the fully saturated vacancy, i.e., $x=4c$, $x_4=c$, and $x_1=x_2=x_3=x_v=0$, the above Eqs. (14) become

$$N_{\mathrm{Si}}=-\frac{1}{\pi}\mathrm{Im\,Tr}\left[(\tilde{\Sigma}-\tilde{\epsilon}_{\mathrm{H}}')\frac{1}{\epsilon_{\mathrm{Si}}-\tilde{\epsilon}_{\mathrm{H}}'}\tilde{G}_e\right] , \tag{15}$$

$$N_{\mathrm{H}}=-\frac{1}{\pi}\mathrm{Im\,Tr}\left[(\tilde{\Sigma}-\tilde{\epsilon}_{\mathrm{Si}})\frac{1}{\epsilon_{\mathrm{H}}'-\tilde{\epsilon}_{\mathrm{Si}}}\tilde{G}_e\right] .$$

These equations can be further reduced to give the $s$- and $p$-like components of the DOS. The total DOS is of course the sum of $N_{\mathrm{Si}}$ and $N_{\mathrm{H}}$. The CPA, as described above, treats the diagonal disorder. The inclusion of off-diagonal disorder in the

TB-CPA is computationally very complicated and at present there is no established "best" technique.

In our calculations, the off-diagonal disorder was treated within the virtual crystal approximation (VCA), i.e., the nearest-neighbor matrix elements were replaced by their averaged values:

$$E_{i,j}(\tfrac{1}{2}\tfrac{1}{2}\tfrac{1}{2})=\left[1-\frac{x}{2}\right]E_{i,j}^{\text{Si-Si}}(\tfrac{1}{2}\tfrac{1}{2}\tfrac{1}{2})+\frac{x}{2}E_{i,j}^{\text{Si-H}}(\tfrac{1}{2}\tfrac{1}{2}\tfrac{1}{2})$$

$$i,j=s,x,y,z \ . \quad (16)$$

The VCA is a good approximation if the difference between the Si-Si and the Si-H matrix elements is small in comparison to their average value. This condition is not satisfied for all matrix elements and so there is a need here for improving our present calculational techniques. Given, however, the complexity of introducing off-diagonal disorder in the CPA and that there are already other uncertainties in our model, we decided in the present stage to work with the VCA for the off-diagonal disorder. We have used the simple CPA (no cluster extensions) and have assumed that there is no statistical correlation among the various configurations discussed before. At this point we must note that it has been proposed that vacancies [see Fig. 1(b)] tend to cluster together as to form microvoids and internal surfaces.[13,39] We have found that this clustering effect effectively reduces the value of $c$ and tends to create some internal surface states which make a small contribution to the total DOS. Thus the vacancy clustering effects can easily be incorporated in our model by appropriately reducing the value of $c$. Let us add that in the presence of adequate hydrogen during the growth process this clustering effect may not occur.

## IV. RESULTS AND DISCUSSION

In Fig. 2 we show the DOS in the gap region for the configuration Si and vacancies with no hydrogen introduced yet. We note the appearance of dangling-bond states in the gap. The density of these states increases with vacancy concentration $c$. Also the gap becomes smaller with increasing $c$ until it is completely filled. It is also interesting to note that the gap states have as their center of gravity the position of the bound state (0.75 eV) of the ideal single vacancy.[20–22] It should be stressed here that the results of Fig. 2 are useful in demonstrating qualitatively the existence of dangling-bond states in the gap. However, due to the omission of the effects of reconstruction, we certainly overestimate the number of these states and, therefore, we don't attempt any quantitative comparison with experiment.

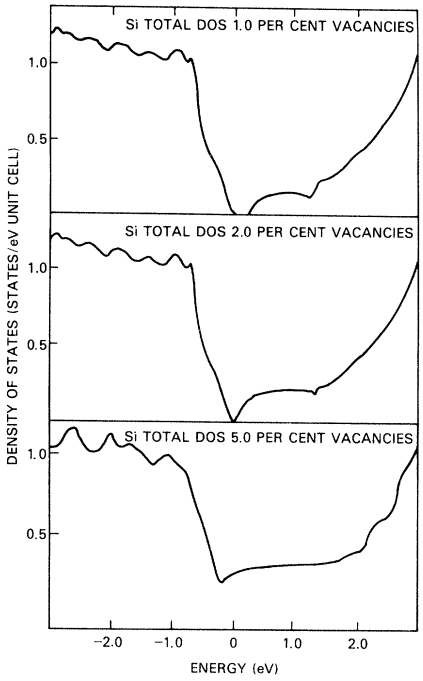


FIG. 2. CPA densities of states in the gap region for the Si vacancy case for different vacancy concentrations.

Figure 3 deals with the restoration of the band gap upon hydrogenation. Figure 3 corresponds to $c=0.05$ and $0\leq x\leq 4c$. It is evident that by in-

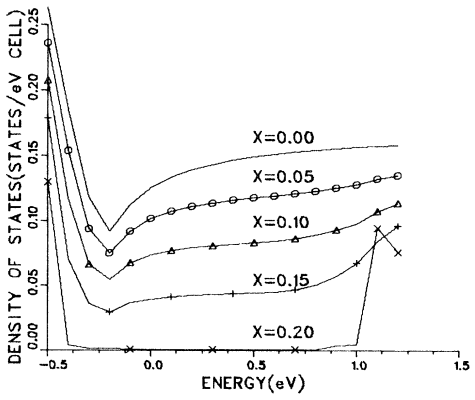


FIG. 3. Densities of states of $SiH_x$ in the gap region for different hydrogen concentrations $x$ ($c=0.05$).

creasing the hydrogen content $x$, the states in the gap are reduced until they are completely eliminated for the fully hydrogen-saturated-vacancy case ($x=0.20$). This is, of course, what the experimental situation is and the reason why $a$-Si:H has semiconducting properties similar to those of crystalline Si.

In Fig. 4 we show the DOS of Si-H (with $c=0.05$ and $x=0.20$) for the whole spectrum, including both the valence and conduction bands. We note first a band gap $E_g=1.4$ eV that is wider by 0.4 eV than the corresponding $E_g=1.0$ eV which our tight-binding Hamiltonian gives for the nonhydrogenated case. This widening of the gap is due to a narrowing of the third DOS peak at the top of the valence band. We have identified this to be the result of a decrease of the difference: $E_{x,y}(\frac{1}{2}\frac{1}{2}\frac{1}{2})-E_{x,x}(\frac{1}{2}\frac{1}{2}\frac{1}{2})$, which is a measure of the $pp\pi$ interaction. This recession of the valence band by 0.4 eV is in excellent agreement with the photoemission experiments of von Roedern *et al.*[9] Figure 4 also shows the DOS decomposed by site. The hydrogen-site DOS shows pronounced peaks at 5.2, 7.6, and 13.5 eV below the Fermi level. Comparison with photoemission data is more appropriately done after smoothing the H-site DOS

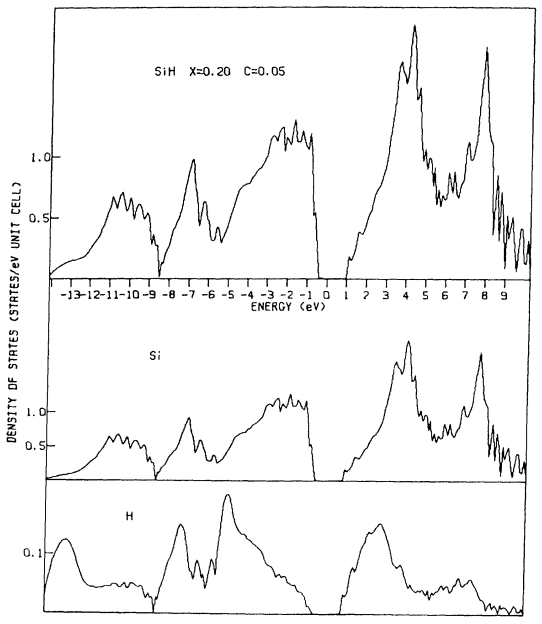


FIG. 4. Total and site-decomposed densities of states for $SiH_x$ with $x=0.2$. Note that the Si and H DOS are multipled by $(1-c)$ and $c$, respectively ($c=0.05$). The Fermi level is located in the middle of the gap.

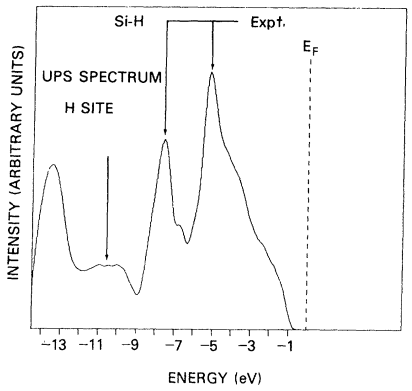


FIG. 5. Broadened H-site density of states. The arrows indicate the peak positions from the photoemission measurements (Ref. 9).

by applying a Lorentzian broadening. This is plotted in Fig. 5 which shows that the 5.2 and 7.6 eV peaks are predicted in almost exactly the same position found in the measurements.[9] The 13.5 eV peak is not seen experimentally for reasons we do not understand.

The widening of the band gap has been demonstrated experimentally by a variety of experimental techniques.[6-8] To compare with these experiments, we have performed a calculation of the joint DOS $N^J(E)$. The calculated $[N^J(E)]^{1/2}$ is assumed to be proportional to the measured quantity $(\alpha E)^{1/2}$, where $\alpha$ is the absorption coefficient. A comparison with the measurements of Cody *et al.*[7] is shown in Fig. 6, where $[N^J(E)]^{1/2}$ has been normalized to the value of $(\alpha E)^{1/2}$ at $E=4$ eV. The experimental graph was obtained at approximately

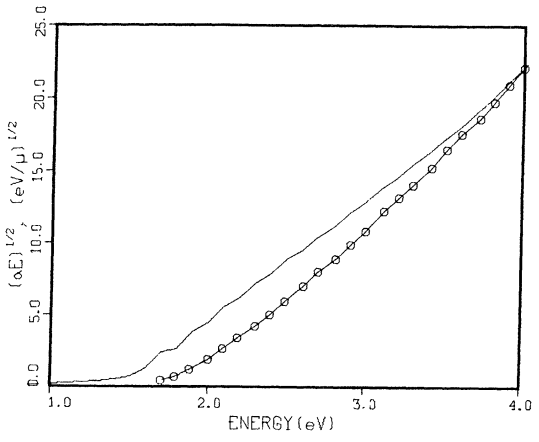


FIG. 6. Plot of the square root of the joint density of states versus energy. The line joining the open circles represents the measured quantity $(\alpha E)^{1/2}$ (Ref. 7).

16% hydrogen content, while the theoretical graph corresponds to 20%. Despite this and the fact that the theory predicts a smaller gap the overall agreement is rather good.

Our calculations can also be used to compare with Auger and soft-x-ray-emission measurements.[40] We present in Fig. 7 a decomposition of the Si-site DOS of SiH in its $s$ and $p$ components. The $s$-like and $p$-like DOS are proportional to the $K$ and $L$ spectra, respectively.

We now turn to a discussion of hydrogen-induced antibonding states at the bottom of the conduction band. Let us first examine the case of a single configuration of the kind shown in Fig. 1(b) embedded in a Si lattice.

The bound states around this four-hydrogen cluster will be given by

$$G_{11}(E)=\frac{1}{E'_{ss}(000)-E_{ss}(000)}\ , \tag{17a}$$

$$G_{22}(E)=\frac{1}{E'_{xx}(000)-E_{xx}(000)}\ . \tag{17b}$$

The graphical solution of Eq. (17a) is shown in Fig. 8. As we see from Fig. 8, there is no real solution of Eq. (17a) because the intersection of Re$G$ with $1/E'-E$ occurs within the band where Im$G\neq 0$. On the other hand, this intersection occurs near the bottom of the conduction band (CB). The physical meaning of no real intersection is that there are no true bound states associated with the four-hydrogen cluster embedded in a Si lattice. The fact that the intersection occurs near the bottom of the CB where Im$G$ is very small means, physically, that the four-hydrogen cluster creates resonance $s$ states i.e., states where the wave function has a peak around the cluster. These resonance states can be viewed as a hybridization of the Si-H $s$-antibonding states with the regular Si states at the bottom of the conduction band. Such resonance states are associated with a lower than the regular CB mobility (because the electron is almost trapped around the hydrogen). Evaluation of Eq. (17b) showed neither bound states of $p$ character nor any resonance states below 3 eV.

The suggestion of Moustakas *et al.*,[10] born out of their photoconductivity measurements that Si-H antibonding states form at the bottom of the conduction band, is strongly supported by the present calculations. This is shown in Fig. 9 where we have plotted the ratio $N_H/N_t$ as a function of $E$. Indeed, this graph, in addition to the peaks in the valence band that we have already discussed, shows a pronounced maximum at the bottom of the CB indicating strong H participation in the formation of these states.

Finally, we will discuss the variation of the gap size $E_g$ with hydrogen content $x$. We define the Fermi level $E_F=(E_c+E_v)/2$ where $E_v$ is the top of the valence band and $E_c$ the bottom of the con-

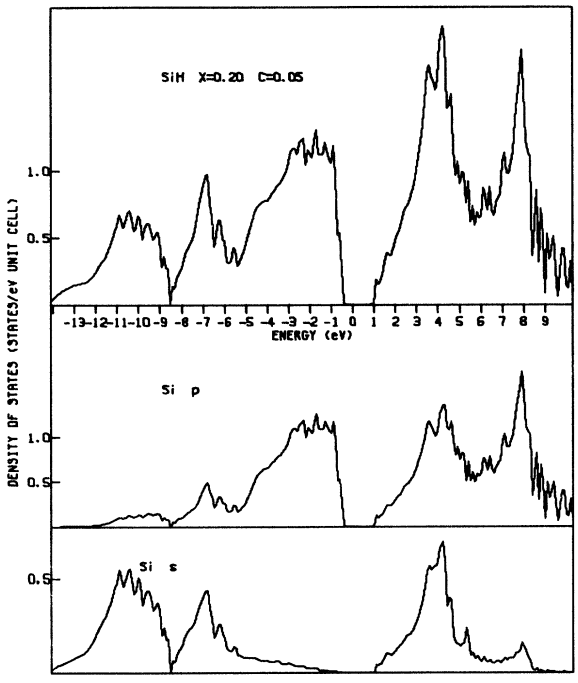


FIG. 7. Si-site density of states and its $s$- and $p$-like components.

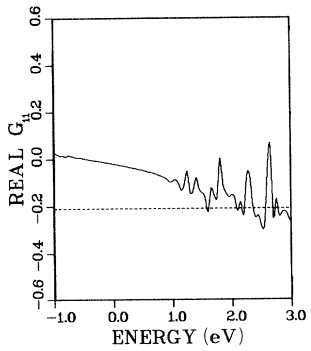


FIG. 8. The real part of the $s$-like Green's function plotted as a function of energy for the case of the single impurity that consists of four hydrogen atoms. The dotted line indicates the value of the right-hand side of Eq. (17a).

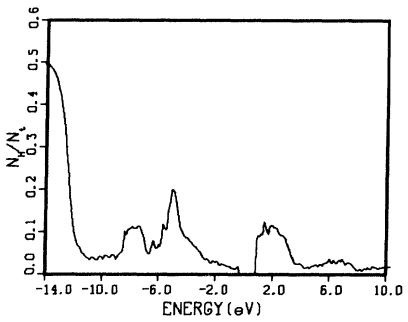


FIG. 9. Ratio of H-site density of states $N_H$ to the total density of states $N_t$ for SiH ($x=0.2$).

duction band. The variation of $E_v$, $E_c$, and $E_F$ with $x$ is shown in Fig. 10, where in all cases we are dealing with vacancies fully saturated by hydrogen, i.e., $x=4c$. We note first that $E_c$ is essentially constant. This is due to a cancellation of the effects of disorder (tends to push $E_c$ down) by the effect of a stronger Si—H bond (tends to push $E_c$ up) as manifested by the larger value of the parameter $\gamma_3$ (see Appendix) in $SiH_x$. $E_v$ depends mainly on the matrix element difference $\gamma_6-\gamma_5$ or equivalently $E_{x,y}(\frac{1}{2}\frac{1}{2}\frac{1}{2})-E_{x,x}(\frac{1}{2}\frac{1}{2}\frac{1}{2})$ which is a measure of the $pp\pi$ interaction. Hydrogen decreases $\gamma_6-\gamma_5$ and so pushes $E_v$ down and widens the gap. As a result $E_F$ is also pushed down.

Our work shows that the size of the gap depends essentially on two parameters: the bond strength $\gamma_3$ and the $pp\pi$ interaction $\gamma_6-\gamma_5$. Hydrogen incorporation effectively increases $\gamma_3$ and decreases $\gamma_6-\gamma_5$ thus producing a wider gap. This effect of

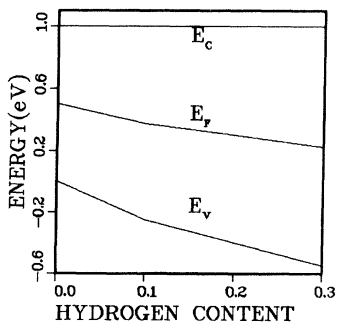


FIG. 10. Variation of the bottom of the conduction band $E_c$ of the Fermi level $E_F$ and the top of the valence band $E_v$ versus hydrogen content for fully hydrogenated samples.

hydrogenation on $\gamma_3$ and $\gamma_6-\gamma_5$, being essentially a local chemical effect, is expected to transcend the validity of our present model and thus constitutes a general feature of hydrogen incorporation in a Si tetrahedral structure.

In conclusion many important properties of fully hydrogenated $a$-Si (such as widening of the gap, Si-H bonding states, Si-H antibonding resonance states) depend mainly on the local chemical environment. Thus these properties are largely independent of the particular model, provided that it satisfactorily treats the limiting case of nonhydrogenated Si. Our present model satisfies these requirements (with the exception of the omission of topological disorder) and as a result we expect our main conclusions to have a much wider validity than the model itself.

## ACKNOWLEDGMENTS

We wish to thank Dr. W. E. Pickett, Dr. L. L Boyer, and Dr. B. M. Klein for many useful discussions and suggestions regarding the calculations. We also thank Dr. T. D. Moustakas, Dr. P. C. Taylor, and Professor W. Paul for discussions regarding the experimental situation. Technical assistance from Mrs. L. Blohm and Mr. A. Koppenhaver is gratefully acknowledged. This work was supported in part by the Solar Energy Research Institute via an interagency agreement between the U. S. Naval Research Laboratory and the U. S. Department of Energy.

## APPENDIX: ESTIMATE OF HYDROGEN-HYDROGEN AND HYDROGEN-SILICON MATRIX ELEMENTS

For each Si we have the four orbitals $|s\rangle$, $|x\rangle$, $|y\rangle$, $|z\rangle$ or equivalently the four $sp^3$ hybridized orbitals shown in Fig. 1(a). The transformations from the one set to the other are the following:

$$\begin{pmatrix}|1\rangle\\|2\rangle\\|3\rangle\\|4\rangle\end{pmatrix}=S\begin{pmatrix}|s\rangle\\|x\rangle\\|y\rangle\\|z\rangle\end{pmatrix}, \tag{A1}$$

$$\begin{pmatrix}|s\rangle\\|x\rangle\\|y\rangle\\|z\rangle\end{pmatrix}=S\begin{pmatrix}|1\rangle\\|2\rangle\\|3\rangle\\|4\rangle\end{pmatrix}, \tag{A2}$$

for the Si at $A$. For the Si at $B$ assuming that $AB$ is along the 111 direction, we have

$$\begin{pmatrix} |5\rangle \\ |6\rangle \\ |7\rangle \\ |8\rangle \end{pmatrix} = \bar{S} \begin{pmatrix} |\bar{s}\rangle \\ |\bar{x}\rangle \\ |\bar{y}\rangle \\ |\bar{z}\rangle \end{pmatrix} , \tag{A3}$$

$$\begin{pmatrix} |\bar{s}\rangle \\ |\bar{x}\rangle \\ |\bar{y}\rangle \\ |\bar{z}\rangle \end{pmatrix} = \bar{S}^T \begin{pmatrix} |5\rangle \\ |6\rangle \\ |7\rangle \\ |8\rangle \end{pmatrix} , \tag{A4}$$

where $\bar{S}^T$ is the transposed matrix of $\bar{S}$. The $4\times4$ matrices $S$ and $\bar{S}$ are given by

$$S = \frac{1}{2} \begin{pmatrix} 1 & 1 & 1 & 1 \\ 1 & 1 & -1 & -1 \\ 1 & -1 & 1 & -1 \\ 1 & -1 & -1 & 1 \end{pmatrix} , \tag{A5}$$

$$\bar{S} = \frac{1}{2} \begin{pmatrix} 1 & -1 & -1 & -1 \\ 1 & -1 & 1 & 1 \\ 1 & 1 & -1 & 1 \\ 1 & 1 & 1 & -1 \end{pmatrix} . \tag{A6}$$

Following the SK notation, the diagonal and nearest-neighbor matrix elements of the Hamiltonian in the $|s\rangle, |x\rangle, |y\rangle, |z\rangle$ representation are denoted as follows:

$$E_{s,s}(000) = \langle s | H | s \rangle , \tag{A7}$$

$$E_{x,x}(000) = \langle x | H | x \rangle = \langle y | H | y \rangle = \langle z | H | z \rangle , \tag{A8}$$

$$E_{s,s}(\tfrac{1}{2}\tfrac{1}{2}\tfrac{1}{2}) = \langle s | H | \bar{s} \rangle , \tag{A9}$$

$$E_{s,x}(\tfrac{1}{2}\tfrac{1}{2}\tfrac{1}{2}) = \langle \bar{x} | H | s \rangle = -\langle \bar{s} | H | x \rangle = \langle \bar{y} | H | s \rangle = \cdots , \tag{A10}$$

$$E_{x,x}(\tfrac{1}{2}\tfrac{1}{2}\tfrac{1}{2}) = \langle \bar{x} | H | x \rangle = \langle \bar{y} | H | y \rangle = \langle \bar{z} | H | z \rangle , \tag{A11}$$

$$E_{x,y}(\tfrac{1}{2}\tfrac{1}{2}\tfrac{1}{2}) = \langle \bar{x} | H | y \rangle = \langle \bar{x} | H | z \rangle = \langle \bar{y} | H | x \rangle = \langle \bar{y} | H | z \rangle = \cdots . \tag{A12}$$

Hirabayashi[41] has written the matrix elements of H in the hybrid representation as follows:

$$\gamma_1 = \langle 1 | H | 1 \rangle , \tag{A13}$$

$$\gamma_2 = \langle 1 | H | 2 \rangle , \tag{A14}$$

$$\gamma_3 = \langle 5 | H | 1 \rangle , \tag{A15}$$

$$\gamma_4 = \langle 6 | H | 1 \rangle , \tag{A16}$$

$$\gamma_5 = \langle 6 | H | 3 \rangle , \tag{A17}$$

$$\gamma_6 = \langle 6 | H | 2 \rangle , \tag{A18}$$

where the orbitals $|6\rangle$ and $|2\rangle$ are along antiparallel directions.

Using Eqs. (A1) and (A2) one easily expresses the $\gamma$'s in terms of the $E$'s and vice versa. We have

$$\gamma_1 = \tfrac{1}{4}[E_{s,s}(000) + 3E_{x,x}(000)] , \tag{A19}$$

$$\gamma_2 = \tfrac{1}{4}[E_{s,s}(000) - E_{x,x}(000)] , \tag{A20}$$

$$\gamma_3 = \tfrac{1}{4}[E_{s,s}(\tfrac{1}{2}\tfrac{1}{2}\tfrac{1}{2}) - 6E_{s,x}(\tfrac{1}{2}\tfrac{1}{2}\tfrac{1}{2}) - 3E_{x,x}(\tfrac{1}{2}\tfrac{1}{2}\tfrac{1}{2}) - 6E_{x,y}(\tfrac{1}{2}\tfrac{1}{2}\tfrac{1}{2})] , \tag{A21}$$

$$\gamma_4 = \tfrac{1}{4}[E_{s,s}(\tfrac{1}{2}\tfrac{1}{2}\tfrac{1}{2}) - 2E_{s,x}(\tfrac{1}{2}\tfrac{1}{2}\tfrac{1}{2}) + E_{x,x}(\tfrac{1}{2}\tfrac{1}{2}\tfrac{1}{2}) + 2E_{x,y}(\tfrac{1}{2}\tfrac{1}{2}\tfrac{1}{2})] , \tag{A22}$$

$$\gamma_5 = \tfrac{1}{4}[E_{s,s}(\tfrac{1}{2}\tfrac{1}{2}\tfrac{1}{2}) + 2E_{s,x}(\tfrac{1}{2}\tfrac{1}{2}\tfrac{1}{2}) + E_{x,x}(\tfrac{1}{2}\tfrac{1}{2}\tfrac{1}{2}) - 2E_{x,y}(\tfrac{1}{2}\tfrac{1}{2}\tfrac{1}{2})] , \tag{A23}$$

$$\gamma_6 = \tfrac{1}{4}[E_{s,s}(\tfrac{1}{2}\tfrac{1}{2}\tfrac{1}{2}) + 2E_{s,x}(\tfrac{1}{2}\tfrac{1}{2}\tfrac{1}{2}) - 3E_{x,x}(\tfrac{1}{2}\tfrac{1}{2}\tfrac{1}{2}) + 2E_{x,y}(\tfrac{1}{2}\tfrac{1}{2}\tfrac{1}{2})] , \tag{A24}$$

$$E_{s,s}(000) = \gamma_1 + 3\gamma_2 , \tag{A25}$$

$$E_{x,x}(000) = \gamma_1 - \gamma_2 , \tag{A26}$$

$$E_{s,s}(\tfrac{1}{2}\tfrac{1}{2}\tfrac{1}{2}) = \tfrac{1}{4}(\gamma_3 + 6\gamma_4 + 6\gamma_5 + 3\gamma_6) , \tag{A27}$$

$$E_{s,x}(\tfrac{1}{2}\tfrac{1}{2}\tfrac{1}{2}) = \tfrac{1}{4}(-\gamma_3 - 2\gamma_4 + 2\gamma_5 + \gamma_6) . \tag{A28}$$

$$E_{x,x}(\tfrac{1}{2}\tfrac{1}{2}\tfrac{1}{2}) = \tfrac{1}{4}(-\gamma_3 + 2\gamma_4 + 2\gamma_5 - 3\gamma_6) , \tag{A29}$$

$$E_{x,y}(\tfrac{1}{2}\tfrac{1}{2}\tfrac{1}{2}) = \tfrac{1}{4}(-\gamma_3 + 2\gamma_4 - 2\gamma_5 + \gamma_6) . \tag{A30}$$

In Fig. 1(b) the Si at $A$ has been removed and four hydrogens have been placed as shown, in order to passivate the Si dangling bonds. Charge-density contours resulting from the pseudopotential supercell calculation of Pickett[35] involving the configuration shown in Fig. 1(b), demonstrate that there are hydrogen $p$ and even $d$ components in the eigenfunction. Furthermore, these charge-density contours strongly suggest that this multiple $l$ hydrogen state can be approximated by an $s$-only or-

bital which is displaced towards the Si site by about 20% as shown in Fig. 1(b). If $0_{1'}$, $0_{2'}$, $0_{3'}$, and $0_{4'}$ are the positions of the centers of the displaced hydrogen $s$ orbitals $|1'\rangle$, $|2'\rangle$, $|3'\rangle$, and $|4'\rangle$, respectively, the distances are as follows: $B0_{1'}=2.30$ a.u., $B0_{2'}=5.18$ a.u., $0_{1'}0_{2'}=3.50$ a.u.

Comparing Figs. 1(a) and 1(b) we can see that the role of the four $sp^3$ hybrids $|1\rangle$ to $|4\rangle$ is played by the four orbitals $|1'\rangle$ to $|4'\rangle$. The result of this replacement is to change the $\gamma_1,\gamma_2,\ldots,\gamma_6$ to $\gamma_1',\ldots,\gamma_6'$ given by

$$\gamma_1'=\langle 1'|H|1'\rangle\ , \tag{A31}$$

$$\gamma_2'=\langle 1'|H|2'\rangle\ , \tag{A32}$$

$$\gamma_3'=\langle 5|H|1'\rangle\ , \tag{A33}$$

$$\gamma_{4(1)}'=\langle 6|H|1'\rangle\ , \tag{A34}$$

$$\gamma_{4(2)}'=\langle 5|H|2'\rangle\ , \tag{A35}$$

$$\gamma_5'=\langle 6|H|3'\rangle\ , \tag{A36}$$

$$\gamma_6'=\langle 6|H|2'\rangle\ . \tag{A37}$$

A complication associated with the configuration of Fig. 1(b) is that $\gamma_{4(1)}'$ and $\gamma_{4(2)}'$ are not necessarily equal as in the configuration of Fig. 1(a). However, as we shall see below the difference between $\gamma_{4(1)}'$ and $\gamma_{4(2)}'$ turns out to be small, thus we can replace these matrix elements by their mean value, i.e.,

$$\gamma_4'=\frac{\gamma_{4(1)}'+\gamma_{4(2)}'}{2}\ . \tag{A38}$$

Before we proceed with the estimation of the values of the $\gamma'$'s we mention that we can introduce fictitious $s$ and $p$ orbitals $|s'\rangle$, $|x'\rangle$, $|y'\rangle$, $|z'\rangle$ associated with four hydrogens of Fig. 1(b) through the relation

$$\begin{pmatrix}|s'\rangle\\|x'\rangle\\|y'\rangle\\|z'\rangle\end{pmatrix}=S\begin{pmatrix}|1'\rangle\\|2'\rangle\\|3'\rangle\\|4'\rangle\end{pmatrix}\ . \tag{A39}$$

These orbitals allow us to define hydrogen associated $E'$'s by replacing in Eqs. (A7)–(A12) the $|s\rangle,|x\rangle,|y\rangle,|z\rangle$ by $|s'\rangle,|x'\rangle,|y'\rangle,|z'\rangle$. Because the transformation in Eq. (A39) is identical to that in Eq. (A2), it follows that the $E'$'s are given in terms of $\gamma'$'s as in Eqs. (A25) and (A30). Thus the removal of a Si and the placement of four hydrogens as shown in Fig. 1(b) is equivalent to changing the six matrix elements $E$'s to the new values $E'$'s. Actually, the second- and third-nearest-neighbor matrix elements should be modified as well. These modifications are difficult to estimate and are not expected to be as important as the changes in the diagonal and nearest-neighbor matrix elements. For these reasons we have omitted these modifications.

We now proceed to estimate the $\gamma'$'s. The quantity $\gamma_1'$ is taken equal to its value in the $SiH_4$ molecule[42]

$$\gamma_1'=-3.38\ \text{eV}\ . \tag{A40}$$

To estimate $\gamma_2'$ we need to obtain the off-diagonal matrix element between the orthogonalized hydrogenic wave functions associated with the configuration shown in Fig. 1(b). Mattheiss[43] has examined this problem in detail for a system of six hydrogens placed in the corners of a canonical hexagon. We think that the nearest-neighbor matrix elements do not depend so sensitively on the geometry and consequently Mattheiss's results can be used to obtain a fair estimate of $\gamma$. We have fitted Mattheiss's results for separations $R=2$, 3, 5 a.u. with a quadratic function times the exponential function $[\exp(-R)]$. We found from this fitting that

$$\gamma_2'=-27.07(1.491-0.072R+0.077R^2)e^{-R} \tag{A41}$$

in units of eV which for $R=3.5$ a.u. gives

$$\gamma_2'=-1.78\ \text{eV}\ . \tag{A42}$$

To obtain $\gamma_3'$ we shall write it by employing Eq. (A3) as follows:

$$\gamma_3'=\tfrac{1}{2}(\langle\bar{s}|H|1'\rangle-3\langle\bar{x}|H|1'\rangle)\ . \tag{A43}$$

Chadi[44] has found that the nonorthogonalized orbital $|\bar{s}_n\rangle$ to which $|\bar{s}\rangle$ reduces as the overlap goes goes to zero is proportional to $R\exp(-1.04R)$. The fact that this $s$ Si decays almost exactly like a hydrogen $s$ orbital suggests that Eq. (A41) may be used to obtain $\langle\bar{s}|H|1'\rangle$. However, the extra factor of $R$ in $|\bar{s}_n\rangle$ would cause the matrix element to decay more slowly than the right-hand side of Eq. (A41). To take this into account we write, in eV

$$\langle\bar{s}|H|1'\rangle=-\frac{V_{\text{Si-H}}}{V_{\text{H-H}}}27.07(1.491-0.072R+0.077R^2)e^{-R}\ , \tag{A44}$$

where

$$V_{\text{Si-H}} = -\left[(\sqrt{3}/4 + 1\sqrt{3})(1+R) + \frac{R^2}{3\sqrt{3}}(2+R/4)\right]\exp(-R)$$

is the off-diagonal matrix element between $\exp(-R)$ and $R\exp(-R)$ and

$$V_{\text{H-H}} = -(1.5+1.5R+R^2/6)\exp(-R)$$

is the same matrix element between two hydrogenic wave functions. To check the accuracy of Eq. (A44) we substitute for $R$ the Si—H distance in $SiH_4$ ($R=2.8$ a.u.) and we obtain $-3.58$ eV. This is in surprisingly good agreement with the established[42] value of $-3.57$ eV. To obtain $\langle \bar{x} \mid H \mid 1' \rangle$ we take into account that the nonorthogonalized $\mid \bar{x}_n \rangle$ is proportional to $x \mid \bar{s}_n \rangle$. Hence it is plausible to write

$$\langle \bar{x} \mid H \mid 1' \rangle = -cR_x \langle \bar{s} \mid H \mid 1' \rangle \ , \tag{A45}$$

where $R_x$ is the $x$ component of the vector $0_{1'}B$, and the constant $c$ can be determined from the known values of $\langle \bar{x} \mid H \mid 1' \rangle$ and $\langle \bar{s} \mid H \mid 1' \rangle$ for the $SiH_4$ molecule.[42] We found $c \approx \frac{1}{3}$. Substituting in Eqs. (A44) and (A45) the values $R = 0_{1'}B = 2.3$ a.u. and $R_x = 1.33$ a.u., we obtain $\langle \bar{s} \mid H \mid 1' \rangle = -4.85$ eV and $\langle \bar{x} \mid H \mid 1' \rangle = 2.15$ eV. Thus,

$$\gamma_3' = -5.65 \text{ eV} \ . \tag{A46}$$

The quantity $\gamma_{4(1)}'$ can be written, by employing Eq. (A3), as

$$\gamma_{4(1)}' = \tfrac{1}{2}(\langle \bar{s} \mid H \mid 1' \rangle + \langle \bar{x} \mid H \mid 1' \rangle) = -1.35 \text{ eV} \ . \tag{A47}$$

By employing Eq. (A3) we can rewrite the rest of the $\gamma'$'s as follows:

$$\gamma_{4(2)}' = \tfrac{1}{2}(\langle \bar{s} \mid H \mid 2' \rangle - \langle \bar{x} \mid H \mid 2' \rangle - \langle \bar{y} \mid H \mid 2' \rangle - \langle \bar{z} \mid H \mid 2' \rangle) \ , \tag{A48}$$

$$\gamma_5' = \tfrac{1}{2}(\langle \bar{s} \mid H \mid 3' \rangle - \langle \bar{x} \mid H \mid 3' \rangle + \langle \bar{y} \mid H \mid 3' \rangle + \langle \bar{z} \mid H \mid 3' \rangle) \ , \tag{A49}$$

$$\gamma_6' = \tfrac{1}{2}(\langle \bar{s} \mid H \mid 2' \rangle - \langle \bar{x} \mid H \mid 2' \rangle + \langle \bar{y} \mid H \mid 2' \rangle + \langle \bar{z} \mid H \mid 2' \rangle) \ . \tag{A50}$$

One may attempt to calculate the matrix elements in the right-hand side of Eqs. (A48)—(A50) by using Eqs. (A44) and (A45). However, Eq. (A44) will overestimate the size of the ($\langle \bar{s} \mid H \mid 2' \rangle$) matrix element because of the presence of the hydrogen at 1′ which represents an effective repulsive potential. In Mattheiss's[43] calculation this reduction of the next-nearest-neighbor transfer matrix element is so large that the matrix element becomes almost zero (actually it changes sign and is positive). In the present case, due to the fact that the hydrogen 1′ is closer to Si and that there is the extra $R$ factor in the Si wave function, one expects a smaller reduction of about 50% assuming that only half the space, i.e., the region around the hydrogen at 2′ would contribute to the integral. This crude reasoning suggests that $\langle \bar{s} \mid H \mid 2' \rangle$ is roughly half the value given by Eq. (A44), i.e.,

$$\langle \bar{s} \mid H \mid 2' \rangle = -0.42 \text{ eV} \ . \tag{A51}$$

The other matrix elements entering Eqs. (A48)—(A50) can be estimated by employing Eq. (A45) and the fact that the vector $2'B$ and $3'B$ are (1.327, 3.799, 3.799) and (3.799, 1.327, 3.799), respectively. We obtain thus

$$\langle \bar{y} \mid H \mid 3' \rangle = \langle \bar{x} \mid H \mid 2' \rangle = 0.19 \text{ eV} \ , \tag{A52}$$

$$\langle \bar{x} \mid H \mid 3' \rangle = \langle \bar{z} \mid H \mid 3' \rangle = \langle \bar{y} \mid H \mid 2' \rangle = \langle \bar{z} \mid H \mid 2' \rangle = 0.53 \text{ ev} \ , \tag{A53}$$

which give

$$\gamma_{4(2)}' = -0.84 \text{ eV} \ , \tag{A54}$$

$$\gamma_5' = -0.11 \text{ eV} \ , \tag{A55}$$

$$\gamma_6' = 0.23 \text{ eV} \ . \tag{A56}$$

Using Eq. (A38) we obtain for $\gamma_4'$

$$\gamma_4' = -1.10 \text{ eV} \ . \tag{A57}$$

The corresponding $E'$'s are obtained from Eqs. (A25)—(A30),

$$E'_{s,s}(000) = -8.72 \text{ eV} \ ,$$

$$E'_{x,x}(000) = -1.60 \text{ eV} \ ,$$

$$E'_{s,s}(\tfrac{1}{2}\tfrac{1}{2}\tfrac{1}{2}) = -3.05 \text{ eV} \ ,$$

$$E'_{s,x}(\tfrac{1}{2}\tfrac{1}{2}\tfrac{1}{2}) = 1.96 \text{ eV} \ ,$$

$$E'_{x,x}(\tfrac{1}{2}\tfrac{1}{2}\tfrac{1}{2}) = 0.64 \text{ eV} \ ,$$

$$E'_{x,y}(\tfrac{1}{2}\tfrac{1}{2}\tfrac{1}{2}) = 0.98 \text{ eV} \ .$$

[1]W. E. Spear and P. G. LeComber, Solid State Commun. 17, 1193 (1975).
[2]W. Paul, A. J. Lewis, G. A. N. Connell, and T. D. Moustakas, Solid State Commun. 20, 969 (1976).
[3]T. D. Moustakas, J. Electron. Mater. 8, 391 (1979).
[4]H. Fritzsche, Sol. Energy Mater. 3, 447 (1980).
[5]T. Tiedje, T. D. Moustakas, and J. M. Cebulka, Phys. Rev. B 23, 5634 (1981).
[6]E. C. Freeman and W. Paul, Phys. Rev. B 20, 716 (1979).
[7]G. D. Cody, C. R. Wronski, B. Abeles, R. B. Stephens, and B. Brooks, Sol. Cells 2, 227 (1980).
[8]N. B. Goodman, H. Fritzsche, and H. Ozaki, J. Non-Cryst. Solids 35—36, 599 (1980).
[9]B. von Roedern, L. Ley, and M. Cardona, Phys. Rev. Lett. 39, 1576 (1977); B. von Roedern, L. Ley, M. Cardona, and F. W. Smith, Philos. Mag. B40, 433 (1970).
[10]T. D. Moustakas, D. A. Anderson, W. Paul, Solid State Commun. 23, 155 (1977).
[11]M. H. Brodsky, M. Cardona, and J. J. Cuomo, Phys. Rev. B 16, 3556 (1977).
[12]J. C. Knights, G. Lucovsky, and R. J. Nemanich, Philos. Mag. B37, 467 (1978).
[13]W. E. Carlos and P. C. Taylor, Phys. Rev. Lett. 45, 358 (1980).
[14]P. D'Antonio and J. H. Konnert, Phys. Rev. Lett. 43, 1161 (1979).
[15]H. J. Stein, Phys. Rev. Lett. 43, 1030 (1979).
[16]T. A. Postol, C. M. Falco, R. T. Kampwirth, I. K. Schuller, and W. B. Yelon, Phys. Rev. Lett. 45, 648 (1980).
[17]W. E. Spear, Adv. Phys. 26, 811 (1977).
[18]J. C. Phillips, Phys. Rev. Lett. 42, 1151 (1979).
[19]D. Alder, Phys. Rev. Lett. 41, 1755 (1978).
[20]G. A. Baraff and M. Schlüter, Phys. Rev. Lett. 41 892 (1978); Phys. Rev. B 19, 4965 (1978).
[21]J. Bernholc, N. O. Lipari, and S. T. Pantelides, Phys. Rev. Lett. 41, 895 (1978); Phys. Rev. B 21, 3545 (1980).
[22]D. A. Papaconstantopoulos and E. N. Economou, Phys. Rev. B 22, 2903 (1980).
[23]E. N. Economou and D. A. Papaconstantopoulos, Phys. Rev. B 23, 2042 (1981).
[24]D. A. Papaconstantopoulos and E. N. Economou, *Tetrahedrally Bonded Amorphous Semiconductors,* edited by R. A. Street, D. K. Biegelsen, and J. C. Knights (American Institute of Physics, New York, 1981), p. 130.
[25]W. Y. Ching, D. J. Lam, and C. C. Lin, Phys. Rev. Lett. 42, 805 (1979); Phys. Rev. B 21, 2378 (1980).
[26]L. Guttman, W. Y. Ching, and J. Rath, Phys. Rev. Lett. 44, 1513 (1980).
[27]M. H. Cohen, J. Singh, and F. Yonezawa, J. Non-Cryst. Solids 35—36, 55 (1980).
[28]D. C. Allan and J. D. Joannopoulos, Phys. Rev. Lett. 44, 43 (1980); J. D. Joannopoulos, J. Non-Cryst. Solids 35—36, 781 (1980).
[29]G. D. Watkins, *International Conference on Lattice Defects in Semiconductors, Frieburg, Germany, 1974* (Institute of Physics, London, 1975), p. 1.
[30]G. A. Baraff, E. O. Kane, and M. Schlüter, Phys. Rev. Lett. 43, 956 (1979).
[31]N. O. Lipari, J. Bernholc, and S. T. Pantelides, Phys. Rev. Lett. 43, 1354 (1979).
[32]C. T. White and K. L. Ngai, J. Vac. Sci. Technol. 16, 1412 (1979).
[33]K. H. Johnson, H. J. Kolari, J. P. de Neufville, and D. L. Morel, Phys. Rev. B 21, 643 (1980).
[34]L. F. Mattheiss and J. R. Patel, Phys. Rev. B 23, 5384 (1981).
[35]W. E. Pickett, Phys. Rev. B 23, 6603 (1981).
[36]D. P, DiVincenzo, J. Bernholc, M. H. Brodsky, N. O. Lipari, and S. T. Pantelides, *Tetrahedrally Bonded Amorphous Semiconductors,* edited by R. A. Street, D. K. Biegelsen, and J. C. Knights (American Institute of Physics, New York, 1981), p. 156.
[37]P. Soven, Phys. Rev. 156, 809 (1967); S. Kirkpatrick, B. Velicky, and H. Ehrenreich, Phys. Rev. B 1, 3250 (1970).
[38]J. S. Faulkner, Phys. Rev. B 13, 2391 (1976); D. A. Papaconstantopoulos, B. M. Klein, J. S. Faulkner, and L. L. Boyer, *ibid.* 18, 2784 91978).
[39]J. A. Reimer, R. W. Vaughan, and J. C. Knights, Phys. Rev. Lett. 44, 193 (1980).
[40]H. H. Madden, Bull. Am. Phys. Soc. 26, 453 (1981); G. Wiech and E. Zöpf, in *Band Structure Spectroscopy of Metals and Alloys,* edited by D. J. Fabian and L. M. Watson (Academic, New York, 1973), pp. 629—640.
[41]K. Hirabayashi, J. Phys. Soc. Jpn. 27, 1475 (1969).
[42]M. L. Sink and G. E. Juras, Chem. Phys. Lett. 20, 474 (1973); K. C. Pandey, Phys. Rev. B 14, 1557 (1976).
[43]L. F. Mattheiss, Phys. Rev. 123, 1209 (1961).
[44]D. J. Chadi, Phys. Rev. B 16, 3572 (1977).